



Article

3D-printed Guided Mode Resonance Readout System for Biomedical and Environmental Applications

Hironmay Deb^{1,a,*}, Nantarat Srisuai^{2,b}, Sakoolkan Bonruang^{2,c}, Romuald Jolivot^{1,d}, Chamras Promptmas^{3,e}, and Waleed S. Mohammed^{1,f}

¹ Center of Research in Optoelectronics, Communication and Computational Systems (BU-CROCCS), School of Engineering, Bangkok University, Pathum Thani 12120, Thailand

² Opto-Electrochemical Sensing Research Team (OEC), Spectroscopic and Sensing Devices Research Group (SSDRG), National Electronics and Computer Technology Center (NECTEC), Pathum Thani 12120, Thailand

³ Department of Biomedical Engineering, Faculty of Engineering, Mahidol University, Nakhon Pathom 73170, Thailand

E-mail: ^{a*}deb.hironmay@gmail.com, ^bnantarat_kmutt@hotmail.com, ^csakoolkan.boonruang@nectec.or.th, ^dromuald.j@bu.ac.th, ^echamras.pro@mahidol.ac.th, ^fwsoliman@gmail.com

Abstract. This paper demonstrates design and development of an open-source platform-based reflection spectroscopy readout system for guided mode resonance (GMR) sensing applications. The GMR dimensions, reflection grating period, imaging system and components orientations are optimized to enhance the angular resolution while sustaining resonance excitation within the visible range. To achieve the needed arrangement of the multiple components, 3D printing is utilized to build the mechanical mounting. The reflection spectra are extracted from the webcam images and processed using a software written on raspberry-pi computational unit. This ensures the compactness and portability of the system. The system performance of the transducer is tested by measuring the changes in the refractive index of the environment at the GMR chip interface.

Keywords: Guided mode resonance, spectrometer, open-source platform, refractive index sensing, 3D printing.

ENGINEERING JOURNAL Volume 25 Issue 6

Received 22 January 2021

Accepted 28 May 2021

Published 30 June 2021

Online at <https://engj.org/>

DOI:10.4186/ej.2021.25.6.35

1. Introduction

Guided Mode Resonance (GMR) Spectroscopy has been a promising platform for biomedical and environmental sensing for several years [1, 2]. Most of the currently existed GMR based read-out systems for analytes detection use commercial spectrometers [3]. Research now mostly focuses on the integration of GMR transducers with compact spectrometers for real time, point of care and easy to use detections [4]. Several research works have been done in integrating smartphone as an imaging device for spectrometry applications. The use of smartphones for the interest of developing portable, low-cost optical spectroscopic devices have shown a great potential for point of care diagnostics [5-7]. A smartphone sensor-based spectrometer was designed and applied for ultra-violet remote sensing of atmospheric sulphur dioxide by Thomas C. Wilkes et al. using Differential Optical Absorption Spectroscopy method [8]. M. A. Hossain et al. developed a smartphone-based spectrometer and it implemented for dual sensing of absorption and fluorescence of metal ions in water [9]. Their concept of sensing is based on the measurement of absorption in the UV range and fluorescence in the visible range. Another work of M. A. Hossain et al. demonstrated the use of smartphone-based spectrometer using bundled optical fiber for measuring quality of fruit samples [10]. The absorbance was recorded in VIS-near IR spectrum. Few researches focused on GMR based system which can be implemented towards lab-on chip technology aiming for possible integration with smartphone or any imaging and processing device. A chirped GMR based biosensor was proposed for parallel detection of multiple protein biomarkers in human urine [11]. The combined sensing and imaging capability of the chirped GMR biosensor replaces the need for bulky and expensive spectrometer. H.A. Lin et al. proposed a gradient grating period GMR filter is proposed for integration with smartphone [12].

The advantages of using smartphones intrinsic sensors such as camera to be used as a diagnostic tool are compelling. This however brings several challenges. With smartphone companies manufacturing a wide range of phones having different specifications, building an all-in-one smartphone-based biosensor is difficult. It is more convenient to focus on one model. As an alternative, open-source microcontroller such as Arduino and Raspberry Pi can be used as a generic platform of diagnostic for biomedical and environmental applications as compared to traditional systems [13, 14]. The small sized unit with capabilities on computation, communication and networking combined with user friendly interface could be the next option for designing readout systems [15, 16].

In this paper, a GMR based optical read out system using off-the-shelf components based on open-source technology and 3D printing technique is presented. This aims to be a possible platform for developing affordable reflection spectrometer-based readout system. This can be applied for several optical sensors not restricted only to

GMR. Here, the read-out system is constrained to operate in the visible region of the spectrum (450nm-650nm) in order to utilize the emission spectrum of off-shelf white LED source. Accordingly, the GMR chip is designed to have a resonance in the green and red ranges of the visible spectrum for air and solution superstrates respectively. The chips are fabricated using an in-house built Laser Interference Lithography (LIL) and nanoimprint technique. This reduces the cost and complexity of the fabrication process. The developed spectrometer is built using a metal coated grating fabricated with LIL technique and Plasma-enhanced chemical vapor deposition (PECVD). The reflected spectrum is captured by a CMOS camera and analysed by an image processing algorithm to detect the resonance peak location on a Raspberry Pi using a code written in Python. Fused Deposition Modelling 3D printing technique is used to fabricate the entire read-out system of the sensor to ensure the desired alignments of the different components. 3D printing plays a very important role in the system development due to the critical mechanical alignment that is required to achieve the desire spectrometer. It also provides an efficient and fast prototyping technique especially when the design parameters need to be optimized for the targeted performance. The system is tested based on refractive index (RI) change in the cover of the GMR transducer by using solutions of different refractive indices.

In principle the GMR structure consists of a subwavelength grating and a waveguiding layer as shown in Fig. 1(a). Resonance occurs when meeting a phase matching condition between guided modes and a diffracted order inside the structure. The mode coupled by the grating is then re-radiated back through constructive interference of the leakage from the grating. Neglecting material loss, at resonance, a strong reflection with high spectral and angular selectivity is obtained. Peak reflection, or dip in transmission, spectrum is produced as shown in Fig. 1(b). Resonance condition is affected by modal properties of the guiding region (the effective index n_{eff}), excitation wavelength (or Peak Wavelength Value, PWV) and the refractive index on the surface of the sensor (n_{sup}). This effect is visualized in Fig. 1(b) when changing the superstrate index from n_{sup1} to n_{sup2} . Such refractive index sensing principle has been used in various fields including chemical analysis, medical diagnostics and environment monitoring [17-19].

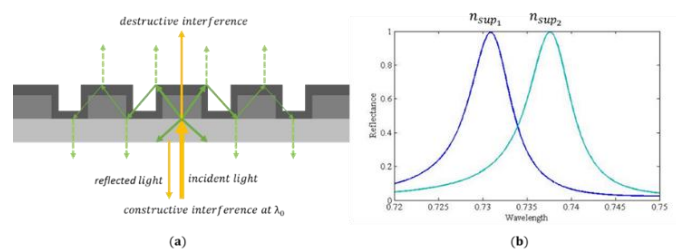


Fig. 1. (a) Guided Mode Resonance (b) Shift in resonance with change in refractive index.

The paper focuses here on building a platform fully based on open-source resources and 3D printing to utilize the GMR response towards sensing applications. The following sections present the different components of the read-out system and the design approach. The paper is divided into two sections: The proposed read-out system and the implementation of the read-out system for sensing applications. In section three the system is tested with solutions of different refractive indices and its response is calculated.

2. Proposed Read-Out System

The schematic of the proposed GMR transducer integrated with an in-house built spectrometer designed using off-shelf components is shown in Fig. 2.1. The design of the proposed system is divided in three parts: light excitation and collection from the GMR transducer, integrated reflection spectrometer and peak value tracking based on algorithm using Raspberry Pi. Warm white light source is used to illuminate the GMR chip, which is designed to reflect a specific waveband depending on the refractive index of the environment at the GMR interface. This reflection is then diffracted by a reflection grating into wavelength dependent angular components which are acquired by an imaging device. Image processing algorithm is implemented in Python on a Raspberry pi in order to extract the reflection spectrum and peak detection. The peak wavelength of the reflection shifts depending on the refractive index of the sample at the GMR interface. The system is then calibrated by applying a range of samples with a known refractive index and measuring the peak shift.

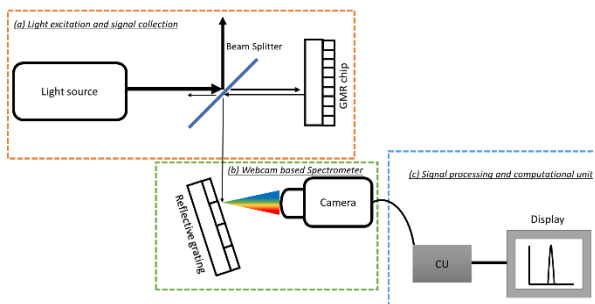


Fig. 2.1 Schematic of the proposed system (a) Light excitation and signal collection (b) Webcam based Spectrometer (c) Signal processing and computation unit (CU)

2.1. Light Excitation and Collection from GMR Transducer

Light excitation of the GMR system is done using a warm white (300 K) LED source (OSLON Square 3rd generation) with an LED driver (LUMOTECH, LO5050,1-6.5 Watt, 700mA). A linear polarizer is placed to allow only Transverse Magnetic (TM) light to be incident at the bottom of the GMR chip. TM polarized light results in a narrow resonant linewidth that results in an enhanced limit of detection (LOD) [20]. The spectral

tunability of the resonance peak can be analysed using Rigorous Coupled Wave Analysis (RCWA) simulations [21, 22]. The tunability is calculated numerically by changing the key geometrical parameters of the device.

The key design parameters in determining the spectral position of the GMRs are the thickness of the grating region and the period of the grating. The main aim is to keep the resonance within the visible region (450nm to 650 nm) in order to match the emission spectrum of the light source. The sensitivity of the GMR is however proportional to its period. Increasing the period shifts the resonance to higher wavelengths and this leads to low excitation power due to operation at the edge of the emission spectrum. To keep the resonance peak location within the visible range, the GMR structural parameters are varied using RCWA. In the calculations, the simulated device is estimated to be a rectangular slab structure of one-dimensional grating. In practice, the grating master is fabricated using laser interference lithography where the final grating is imprinted on a spin-on-glass (SOG) layer with refractive index $n_{gf}=1.4$. In Fig. 2.2, Λ is the period, t_g is the grating depth, t_f is the thickness of Tantalum Pentoxide (Ta_2O_5) layer, with refractive index $n_f=2.1$, that acts as a waveguiding layer and t_{gf} is the thickness of the film under the grating. In all the calculations in Fig. 2.2, water as ($n_{sup} = 1.33$) superstrate is considered.



Fig. 2.2 Structure of GMR simulated in RCWA.

To optimize the structure for operation in the visible region, three grating periods were selected: 330nm, 350nm and 370nm. The depth of the grating was varied from 100 to 200nm. A thinner waveguiding layer allows only the fundamental mode to be guided. That results in a single resonance peak. Figure 2.3 shows the contour plot of the variation in resonance peak with change in tuning parameters for the fundamental mode. The tuning of the structure was done in RCWA to select optimized parameters.

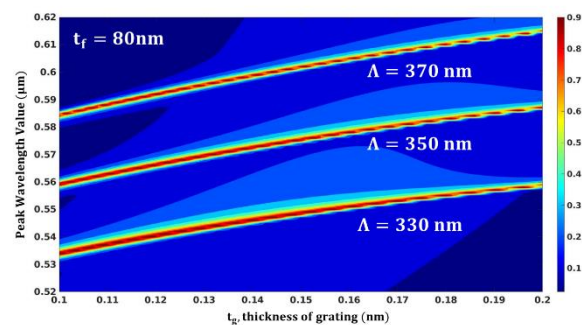


Fig. 2.3 Contour plot of Resonance Peak variation for $\Lambda=330$ nm, $\Lambda=350$ nm and $\Lambda=370$ nm with t_g varied from 100-200nm.

For the considered GMR parameters, Fig. 2.2 indicates that a period of 350nm, $t_{gf}=180\text{nm}$ and $t_g=80\text{nm}$ with a filling factor of 0.5 provides peak wavelength within the green-red visible spectrum range. Hence, these parameters are selected for the GMR fabrication.

2.2. Design approach of the integrated spectrometer

For the detection of the designed GMR chip, a simple in-house built spectrometer is used. The main concept of the spectrometer design is to maximize the angular spectrum of the first or second order diffraction to cover the entire image sensor area of the CMOS camera. The in-house spectrometer is composed of a reflective grating (made by coating an imprinted dielectric grating with a thin film of Chromium) and a webcam (ELP-USB8MP02G-L75, Ailipu Technology Co., Ltd, China). The reflected signal from the GMR chip is incident on the grating through a narrow slit (around 1 mm width) at an angle θ_i . It is then separated into wavelength dependent angular components that is captured by the camera. In order to achieve a compact design, the imaging system comprising of one lens and a CMOS camera is arranged to maximize the coverage width of the visible spectrum covering the whole extent of the image sensor as shown in Fig. 2.4.

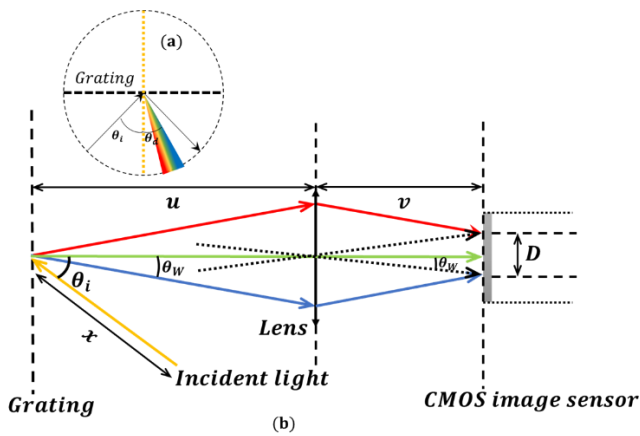


Fig. 2.4 Diffraction of light into angle θ_d from the grating

In Fig. 2.4, θ_i and θ_d are the incident and diffraction angles.

$$\theta_d = \sin^{-1} \left[m \left(\frac{\lambda}{\Lambda} \right) - \sin \theta_i \right] \quad (1)$$

where, m is the order of diffraction. θ_d is dependent on λ and inversely dependent on Λ . The angular width θ_w is the difference between diffraction angles of red, $\theta_{d,r}$ (at $\lambda = 450 \text{ nm}$), and blue, $\theta_{d,b}$ (at $\lambda = 650 \text{ nm}$), $\theta_w = \theta_{d,r} - \theta_{d,b}$. The influence of the angular width on the spectrometer design is illustrated by the ray tracing of the imaging system as shown in Fig. 2.4 when D equals the CMOS image sensor width. The effect of the grating

period on the angular width, w , is shown in Fig. 2.5 for both first order and second order diffraction. Here, grating periods from 950 nm to 1250 nm are considered. This is due to the availability of reflection gratings around 1000 nm period.

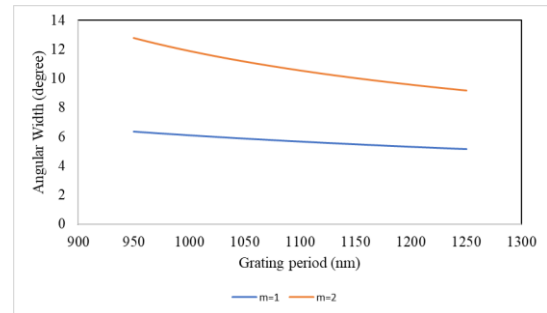


Fig. 2.5 Angular width calculation for grating period from 950-1250 nm for $m=1$ and $m=2$ order of diffraction.

In the designed spectrometer the recorded image is a correlation between the aperture image and the desired spectrum. This image is captured by the CMOS camera. Hence, the imaging system needs to de-magnify the aperture in order to enhance the resolution however it needs to maximize the coverage area of the spectrum image. Using the geometry in Fig. 2.4, the imaging distance needed to cover a distance D on the image sensor is

$$v = \left(\frac{1}{\tan \theta_w} \right) \times D/2 \quad (2)$$

where D is the width of the image sensor. Using thin lens equation for a lens of a focal length f , $1/f = 1/v + 1/d$, and an object distance $d = x + u$, where x is the distance from the source to the grating, the magnification m can be calculated as

$$m = \frac{D/2 - (\tan \theta_w f)}{(\tan \theta_w f)} \quad (3)$$

The image area of the CMOS camera is 6.18 mm x 5.85 mm with a maximum resolution of 8-megapixel (3264(H)x2448(V)) with a pixel size of $1.4\mu\text{m}$. Three different lenses were provided with the camera: 6 mm, 8mm or 12 mm. The object distances for the three lenses are calculated and shown in Fig. 2.6 a). As shown, larger focal length results in larger object distance and hence lower magnification is obtained. That results in a better resolution of the spectrum image. Selecting 12 mm focal length, the magnification and the number of pixels covered by the image is shown in Fig. 2.6(b). Based on the simulated design parameters, a grating period of 1200 nm is chosen for fabricating the reflective grating. The mechanical alignment of the read-out system is provided using 3D printed structures. Fused Deposition Modelling technique is used for making 3D printed support structures [23].

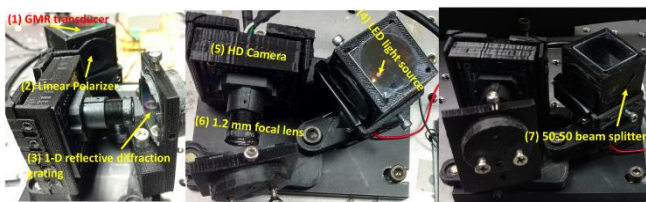


Fig. 2.7 Realized GMR based system with spectrometer along with components assemblies using 3D printed parts.

Figure 2.7 shows the realized GMR based read-out system with the following components as labelled in the figure: (1) GMR transducer, (2) a linear polarizer, (3) 1-D reflective grating, (4) a commercial LED light source, (5) an HD camera, (6) 1.2 mm focal lens, (7) 50-50 beam splitter. A linear polarizer sheet is placed to allow only TM polarization. The distance between the beam splitter and the reflective grating is kept at 50 mm and the distance between the grating and lens is set to 15 mm. These distances were selected such that the diffracted spectrum covers almost the whole detection area. The signal acquisition is performed using a CMOS camera which is connected to a Raspberry Pi for detecting the reflection spectrum. The spectrometer is designed based on the parameters mentioned in Table 1.

Table 1. Design parameters for spectrum to capture the 2nd order spectrum for analysis.

Spectrum	θ_w	d	v	m
450nm-650nm	20°	50 mm	15 mm	0.5

2.3 Image processing algorithm for peak value tracking

Using the design approach (section 2.2), the image of the spectrum of the GMR signal that is convolved by the de-magnified aperture is captured by the camera. The captured image is cropped using two manually set tracks, Track 1 and Track 2, as shown in Fig. 2.8(a). The cropped frame covers the spectrum from blue to red. The spectrum and the peak tracking are performed using an image processing algorithm developed using Python Programming language on Raspberry Pi 3.

In extracting the spectrum, first a reference frame is set, which is the reflection from a glass side coated with tantalum pentoxide. For image acquisition from the CMOS camera, the image is acquired several times (six times in the Fig. 2.8) and averaged to increase the signal to noise ratio (SNR). The cropped region between tracks 1 and 2 is then converted grayscale and the value of the pixels are summed vertically to generate the spectrum. This is saved as a reference spectrum. Then the reference chip is removed and the GMR sample is placed instead and the same procedure is applied to generate the raw

GMR spectrum. The recorded value from the GMR sample is then normalized with respect to the reference. The peak detection is achieved by first locating the index of the pixel with maximum value in the normalized spectrum. A small region is then selected around that value (20 pixels for example) where the peak spectrum is fitted to a second order polynomial. The peak value is then refined by detecting the peak of the fitted function. This helps reducing the noise effect and increases the resolution of the detection. The GUI designed to track and record the resonance peak is shown in Fig. 2.8(b).

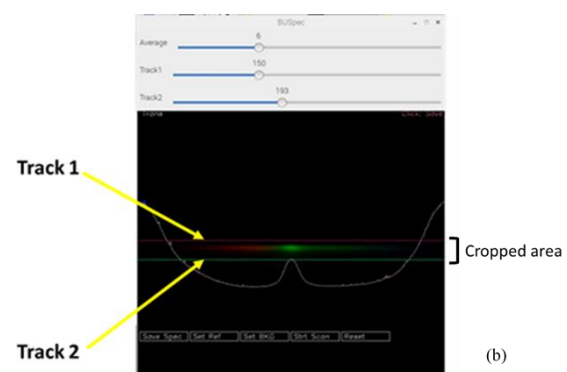
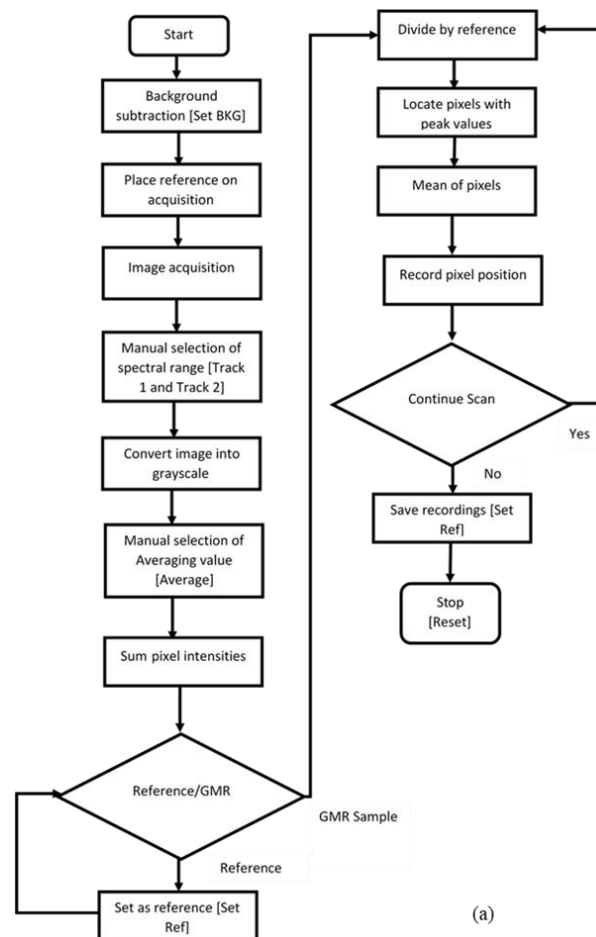


Fig. 2.8 (a) Image processing flowchart of spectrum analysis for extraction of spectral data and finding peak position (b) Graphical User Interface (GUI) for peak tracking.

3. Experimental Results and Discussion

The sensitivity of the readout system was tested with Glycerol solutions of four different RI values. The testing starts with De-ionized water. The sensing surface is then cleaned before the second sample is placed. This process is repeated for sample 3, sample 4 and sample 5. The deviation in the peak position due to the change in the RI of the solution is recorded as delta pixels, taking the position at which, the peak occurs for de-ionized water on the sensing surface as the starting pixel. The peak position for the refractive index ranges from 1.33248 to 1.35417 covered the green to red visible spectrum.

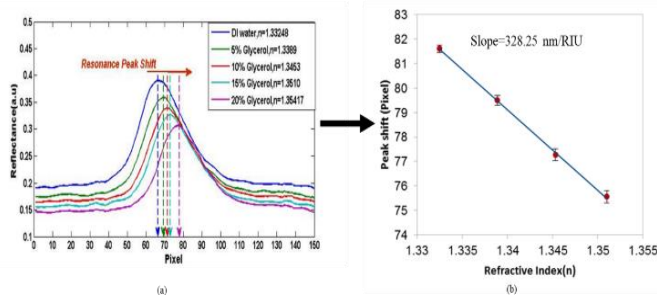


Fig. 3.1 (a) Resonance peak shift for different solutions from experiment. (b) Plot of peak position with change in superstrate refractive index from experiment.

The plot of pixel position with increase of RI along with standard deviation is shown in Fig. 3.1(a). There is a clear shift in the peak position with increase of the solution refractive index. The spectrum is recorded for 15 times for each refractive index with an interval of one minute. Number of recordings is used to calculate the standard deviation of the peak position.

Figure 3.1(b) shows the peak position of different solutions and its standard deviation. The slope of the linear fit gives the sensitivity of the GMR transducer. The theoretical limit of detection (LOD) was determined as the standard deviation (STD) divided by the sensitivity (nm/RIU). Using data, the LOD calculated is 6.093×10^{-4} .

A LOD of the order of 10^{-4} RIU in the visible region is not high compared to commercial sensors. However, it is sufficient in applications where threshold detection is needed of the read-out system [24, 25]. It can be used for detection of organic gases as gas sensor [26], or as biosensor for bulk sensing or surface sensing with appropriate surface functionalization [27]. The spectrometer developed here using off-the-shelf optical components, diffraction grating and applying Raspberry pi as peak tracking tool provides a feasible platform to reduce the need of commercial spectrometers especially when budget is constrained. Optimal conditions for alignment of spectrometer components can be calculated depending upon the webcam specifications as mentioned in this paper. The spectrum for the resonance peak can be varied by changing the period of the grating making it possible for the end user to select the range of spectrum in the

visible region for which the application is to be done. This read-out system also has the flexibility of selecting 1D GMR transducer of different materials [28], different structure [29], or 1-D GMR transducer utilizing higher order modes that have resonance peak within the visible region [30]. Low-cost 3D printing technology provides a robust support to the different optical components. Finally, it is worth mentioning that LOD can be improved through both the GMR structure as well as the read-out system. For example, in earlier work when designing the GMR to work at near cut-off condition, maximum sensitivity was achieved and hence the limit of detection is improved. Another mean to improve LOD is through using a grating with smaller period to increase the angular resolution and hence the resolution of the spectrometer around the spectral range of interest.

4. Conclusion

The developed system using 3D printing technology allows researchers to develop read out systems for refractive index sensing applications. A detection limit of 6.093×10^{-4} which is compatible for threshold limit detection provides a promising platform for implementing the read-out system for several applications. The readout system is based on Raspberry Pi which makes it open source and user friendly. This system can be an ideal candidate for research and academic purposes. The LOD can be improved further by decreasing the standard deviation by using a camera of higher resolution. A lower standard deviation will give a better minimum RIU for detection. Biomedical applications can be realized using this read out system by coating the GMR chip with a chemically active layer that can be used to bind the analyte under test. This system can be further developed for portable and field applications. For threshold detection applications this system can be utilized and further enhanced for applications in real time scenario.

Acknowledgment

The authors would like to acknowledge S&T Postgraduate Education and Research Development Office: PERDO, Center of Excellence on Medical Biotechnology: CEMB, Thailand, for partially supporting this research work.

References

- [1] E. Sader and A. Sayyed-Ahmad, "Design of an optical water pollution sensor using a single-layer guided-mode resonance filter," *Photonic Sensors*, vol. 3, no. 3, pp. 224-230, 2013.
- [2] S. Tabassum, R. Kumar, and L. Dong, "Nanopatterned optical fiber tip for guided mode resonance and application to gas sensing," *IEEE Sensors Journal*, vol. 17, no. 22, pp. 7262-7272, 2017.
- [3] H. Deb *et al.*, "Enhanced sensitivity of guided mode resonance sensor through super-mode excitation at

- near cut-off diffraction,” *Optics & Laser Technology*, vol. 132, p. 106517, 2020.
- [4] J. Choi *et al.*, “Portable, one-step, and rapid GMR biosensor platform with smartphone interface,” *Biosensors and Bioelectronics*, vol. 85, pp. 1-7, 2016.
- [5] A. Roda *et al.*, “Smartphone-based biosensors: A critical review and perspectives,” *TrAC Trends in Analytical Chemistry*, vol. 79, pp. 317-325, 2016.
- [6] L. Kwon *et al.*, “Medical diagnostics with mobile devices: Comparison of intrinsic and extrinsic sensing,” *Biotechnology advances*, vol. 34, no. 3, pp. 291-304, 2016.
- [7] D. Zhang and Q. Liu, “Biosensors and bioelectronics on smartphone for portable biochemical detection,” *Biosensors and Bioelectronics*, vol. 75, pp. 273-284, 2016.
- [8] T. C. Wilkes *et al.*, “Low-cost 3D printed 1 nm resolution smartphone sensor-based spectrometer: Instrument design and application in ultraviolet spectroscopy,” *Optics Letters*, vol. 42, no. 21, pp. 4323-4326 2017.
- [9] M. A. Hossain *et al.*, “Combined ‘dual’ absorption and fluorescence smartphone spectrometers,” *Optics letters*, vol. 40, no. 8, pp. 1737-1740, 2015.
- [10] M. A. Hossain *et al.*, “Optical fiber smartphone spectrometer,” *Optics Letters*, vol. 41, no. 10, pp. 2237-2240, 2016.
- [11] A. Kenaan *et al.*, “Guided mode resonance sensor for the parallel detection of multiple protein biomarkers in human urine with high sensitivity,” *Biosensors and Bioelectronics*, vol. 153, p. 112047, 2020.
- [12] H.-A. Lin *et al.*, “Compact spectrometer system based on a gradient grating period guided-mode resonance filter,” *Optics Express*, vol. 24, no. 10, pp. 10972-10979, 2016.
- [13] T. C. Wilkes *et al.*, “Ultraviolet imaging with low-cost smartphone sensors: Development and application of a raspberry Pi-based UV camera,” *Sensors*, vol. 16, no. 10, p. 1649, 2016.
- [14] K. Bougot-Robin *et al.*, “Optimization and design of an absorbance spectrometer controlled using a raspberry Pi to improve analytical skills,” *Journal of Chemical Education*, vol. 93, no. 7, pp. 1232-1240, 2016.
- [15] T. Nguyen *et al.*, “From lab on a chip to point of care devices: The role of open source microcontrollers,” *Micromachines*, vol. 9, no. 8, p. 403, 2018.
- [16] M. Somarapalli, R. Jolivot, and W. Mohammed, “Realization of low-cost multichannel surface plasmon resonance based optical transducer,” *Photonic Sensors*, vol. 8, no. 4, pp. 289-302, 2018.
- [17] T.-C. Lee *et al.*, “Novel GMR-based biochip,” *Optical Diagnostics and Sensing V*, vol. 5702, pp. 160-167, 2005.
- [18] D. Wawro *et al.*, “Guided-mode resonance sensors for rapid medical diagnostic testing applications,” *Optical Fibers and Sensors for Medical Diagnostics and Treatment Applications IX*, vol. 7173, p. 717303, 2009.
- [19] C.-W. Chang *et al.*, “Resonant wavelength shift detection system based on a gradient grating period guided-mode resonance filter,” *Photonic Fiber and Crystal Devices: Advances in Materials and Innovations in Device Applications XII*, vol. 10755, p. 107550K, 2018.
- [20] Q. Wang *et al.*, “Sensitivity of a label-free guided-mode resonant optical biosensor with different modes,” *Sensors*, vol. 12, no. 7, pp. 9791-9799, 2012.
- [21] M. G. Moharam *et al.*, “Formulation for stable and efficient implementation of the rigorous coupled-wave analysis of binary gratings,” *JOSA A*, vol. 12, no. 5, pp. 1068-1076, 1995.
- [22] M. G. Moharam *et al.*, “Stable implementation of the rigorous coupled-wave analysis for surface-relief gratings: enhanced transmittance matrix approach,” *JOSA A*, vol. 12, no. 5, pp. 1077-1086, 1995.
- [23] K. S. Boparai, R. Singh, and H. Singh, “Development of rapid tooling using fused deposition modeling: A review,” *Rapid Prototyping Journal*, 2016.
- [24] M. C. Estevez, M. Alvarez, and L. M. Lechuga, “Integrated optical devices for lab-on-a-chip biosensing applications,” *Laser & Photonics Reviews*, vol. 6, no. 4, pp. 463-487, 2012.
- [25] P. T. Dang *et al.*, “Guided-mode resonance filter with ultra-narrow bandwidth over the visible frequencies for label-free optical biosensor,” *Journal of Advanced Engineering and Computation*, vol. 3, no. 2, pp. 406-414, 2019.
- [26] L. Guo *et al.*, “Portable organic gas detection sensor based on the effect of guided-mode resonance,” *AIP Advances*, vol. 7, no. 1, p. 015031, 2017.
- [27] B. T. Cunningham and L. Laing, “Microplate-based, label-free detection of biomolecular interactions: Applications in proteomics,” *Expert review of proteomics*, vol. 3, no. 3, pp. 271-281, 2006.
- [28] M. J. Uddin and R. Magnusson, “Highly efficient color filter array using resonant Si₃N₄ gratings,” *Optics express*, vol. 21, no. 10, pp. 12495-12506, 2013.
- [29] C. Ge *et al.*, “Distributed feedback laser biosensor incorporating a titanium dioxide nanorod surface,” *Applied Physics Letters*, vol. 96, no. 16, p. 163702, 2010.
- [30] W. Peng, Y. Chen, and W. Ai, “Higher-order mode photonic crystal based nanofluidic sensor,” *Optics Communications*, vol. 382, pp. 105-112, Elsevier 2017.



Hironmay Deb received his B.Tech (2008) in Electrical and Electronics from Sikkim Manipal Institute of Technology, Sikkim, India and M.Tech (2014) in Electronics and Communication Engineering from Assam Don Bosco University, Assam, India. He is currently a Doctor of Engineering student in Electrical and Computer Engineering at Bangkok University, Pathumthani, Thailand.



Nantarat Srisuai graduated from King Mongkut's University of Technology Thonburi. In 2014, she received her master degree in Physics from the department of Physic, King Mongkut's University of Technology Thonburi, Thailand. As of 2014, she joined Physics graduate program at King Mongkut's University of Technology Thonburi to pursue her doctoral degree. She graduated in 2019 and she is currently working as a researcher assistance at Photonics Technology Laboratory, the National Electronics and Computer Technology research center (NECTEC).



Sakoolkan Boonruang graduated from the department of electrical engineering, King Mongkut Institute of Technology Ladkrabang, Thailand in 1999. In 2002, she joined the college of optics and photonics, CREOL, University of Central Florida, USA, as a graduate student. She received her Ph.D. degree in optics in 2007 with thesis titled "Two-dimensional Guided Mode Resonant Structures for Spectral Filtering Applications" under the supervision of Prof. M. G. Moharam. In the same year, she returned to Thailand and joined the National Electronics and Computer Technology research center (NECTEC), where she is currently a researcher. Her current work focuses on fabrication of one/two dimensional periodical structures, optical sensors, VOCs sensor and biomedical optics applications.



Dr. Romuald Jolivot received a B.Eng degree in Electrical and Electronic Engineering and Computer Vision in 2006 from Université de Bourgogne, France. In 2008, he received a joint Erasmus Mundus Master in Computer Vision and Robotics (ViBot) from Heriot-Watt University (UK), Universitat de Girona (Spain) and Université de Bourgogne (France). He then joined Laboratoire Electronique, Informatique et Image (LE2I) at Université de Bourgogne where he obtained a Ph. D. degree in Instrumentation and Computer Vision in 2011. During 2012-2013, he served as a Postdoctoral Researcher at Photonic Technology Laboratory (PTL) from NECTEC, Thailand where he worked on biomedical imaging project. Since April 2014, he is a research scholar at the School of Engineering at Bangkok University, Thailand. Research interests Computer vision; Image processing; Medical imaging; Multi/hyperspectral imaging; Biomedical instrumentation.



Chamras Promptmas graduated his Diploma in Biotechnology from University of Kent at Canterbury, UK in 1988 and Ph. D. degree in Biochemistry from Mahidol University in 1994. He had worked on biosensor at Mahidol University for more than 15 years. Recently, he joined the department of Biomedical Engineering, Mahidol University as the Director of Biosensors and Micro Total Analysis System Laboratory. He expanded his work to Ion Sensitive Field Effect Transistor (ISFET) and microfluidic systems.



Dr. Waleed S. Mohammed graduated from the department of electronics and electrical communications, Faculty of engineering, Cairo University, Giza, Egypt on 1996 with a major in control systems. In 1997, he joined the Lasers institute (NILES), Cairo University as a teaching assistant. He received M.Sc. degree from the department of computer engineering, Cairo University in 1999. In the same year he joined the College of optics and photonics/CREOL, University of Central Florida, Orlando, FL, USA as a research assistant. In 2001, he received M.Sc. degree in optics in 2001. He completed his Ph.D. work in 2004 and his thesis was titled “nano/micro-optical elements for mode coupling applications. In 2004, he joined Prof. P. W. E. Smith’s ultra-fast photonics laboratory (UPL), Electrical and Computer Engineering department, University of Toronto, as a postdoctoral fellow. In 2005, he joined Prof. Li Qian’s group at the same university. In 2007 Dr. Mohammed joined the International School of Engineering, Chulalongkorn University, Bangkok, Thailand as an instructor in the nano-engineering department. He taught optoelectronics, fundamental of optics, numerical modeling, nano-electronics and research methodology. As of September 2010, He joined the school of Engineering, Bangkok University as a research scholar).